Large Scale Exact Quantum Dynamics Calculations: Using phase space to truncate the basis effectively

Bill Poirier*

Department of Chemistry and Biochemistry, and Department of Physics, Texas Tech University, P.O. Box 41061, Lubbock TX 79409-1061, USA

Abstract

The laws of physics that apply at the molecular scale are the laws of quantum mechanics. Whereas quantum electronic structure calculations are now routine for the most part, "quantum dynamics" calculations of nuclear motion are still plagued with the "curse of dimensionality." Similar challenges may apply to the emerging field of electron dynamics. In this article, the role of recent phase-space (PS) based methods is reviewed—both individually in comparison with each other, and also collectively as an avenue for lifting the above "curse." In addition: (a) the oldest such PS method is revamped, in order to render it suitable for extremely high accuracy applications; (b) a new PS method designed for electron dynamics is applied to a calculation of the He atom—performed in full quantum dimensionality, and treating electron correlation exactly.

 $^{^*}$ Email: bill.poirier@ttu.edu

I. INTRODUCTION

Quantum mechanics is usually regarded as a configuration space (CS) theory. The space on which the wavefunction Ψ "lives" is CS—i.e., $(\mathbf{x}_1, \mathbf{x}_2, \ldots)$, the set of all particle positions, $\mathbf{x}_i = x_{i,\alpha} = (x_i, y_i, z_i)$. The quantum dynamical law governing the time-evolution of $\Psi(\mathbf{x}_1, \mathbf{x}_2, \ldots, t)$ —i.e., the time-dependent Schrödinger equation (TDSE)—is derived as a straightforward Euler-Lagrange equation, from a CS-based Lagrangian action. In most quantum treatments, therefore, the CS or "position space" representation is given a preferred role, either implicitly or explicitly.

Yet, there are many indications that a phase space (PS) approach to quantum theory—encompassing both the position variables, \mathbf{x}_i , as well as their conjugate momenta, $\mathbf{p}_i = p_{i,\alpha} = (p_{x_i}, p_{y_i}, p_{z_i})$, is more natural. The very notion of the "Hamiltonian" for instance—universally recognized as the most important of quantum operators—is an inherently PS notion. The canonical Poisson bracket relation between the \mathbf{x}_i and \mathbf{p}_i —i.e., $\{x_{i,\alpha}, p_{j,\beta}\} = \delta_{ij} \, \delta_{\alpha\beta}$, of crucial importance in classical PS theory—corresponds directly to the equally important canonical commutation relation, $[\hat{x}_{i,\alpha}, \hat{p}_{j,\beta}] = i\hbar \, \delta_{ij} \, \delta_{\alpha\beta} \, \hat{I}$, in quantum theory. Similar comments apply to the Poisson brackets/commutators that govern the time evolution of observables. It is therefore no surprise that three of the earliest and most revered quantum texts that lay out the fundamentals of the correct (post-Schrödinger) theory—i.e., those of Dirac, 1 von Neumann, 2 and Weyl3—all emphasize Hamiltonian or canonical PS aspects.

The PS approach adopted in these "classic" texts is still of great relevance today—particularly in the field of theoretical quantum dynamics, where John C. Light devoted most of his academic career. Examining why and how this is the case is the primary purpose of the present review. To be clear, I use the term "quantum dynamics" (QD) in a broad sense, to incorporate both time-dependent and time-independent (TI) applications. The reason is that complete knowledge of the latter, i.e. of the TI energy eigenstates, enables any solution of the former to be constructed.

Within the field of chemical dynamics, the utility of QD calculations has not always been fully appreciated—owing no doubt to the great success of classical trajectory simulation (CTS) methods⁴ in recent decades. Nevertheless, the importance of quantum effects in many chemical dynamics applications is becoming increasingly acknowledged. The electron transport chain in biological photosynthesis,⁵ for example, gives lie to the assumption that

quantum effects always become "washed" or averaged out as the molecular systems of interest become more complex. It is therefore not surprising that there is an increasing demand for methods that can incorporate QD effects, at least approximately.^{6–8}

Whereas the traditional emphasis within the chemical QD discipline has been to treat just the nuclear motion quantum mechanically, recent years have also seen a rapidly increasing interest in electron dynamics. One reason is advances in attosecond pulse laser technology, which have now made it possible to probe ultrafast electron dynamics experimentally. Theoreticians are struggling to keep up, as most of the established accurate QD (and also electronic structure) technologies are designed for a single (or small number of) adiabatic electronic potential energy surface(s) [PES(s)]. Accordingly, there is a demand for accurate theoretical and computational approaches that can handle non-adiabatic QD well beyond the limits in which the Born-Oppenheimer approximation is valid. In any event, I extend the term "QD" to encompass electron as well as nuclear dynamics.

From a theoretical and computational methodology standpoint, the greatest QD challenge across all of the contexts discussed above remains the oft-discussed "curse of dimensionality": since the dimensionality, f, of CS, grows linearly with the number of particles (i.e., nuclei or dynamical electrons), the space itself (i.e. the number of distinct configurations) grows exponentially. Of course, one strategy for addressing the exponential scaling is to treat quantum effects approximately. In this paper, however, I consider only exact QD methods—i.e., those that in principle converge to exact results with rigorous error bounds, given sufficient computational resources. For exact QD methods to be practical, it is necessary to face the exponential scaling problem head-on.

To this end, a number of different strategies have been employed. In dimensional combination and contraction methods, customized basis sets (often energy-like eigenstates) are precomputed for reduced-dimensional subsystems, and then used to represent the full-dimensional Hamiltonian, \hat{H} .^{11–13} In the multiconfiguration time-dependent Hartree (MCTDH) approach, ¹⁴ the TD wavefunction at each instant in time is decomposed into an optimized sum-of-products form. In the variational self-consistent field (VSCF) approach, ¹⁵ one-dimensional (1D) basis sets are customized for a given system, and then used to generate a full-dimensional direct product basis (DPB) which is subsequently truncated so as to exploit correlations across the $x_{i,\alpha}$ coordinates. While all of these techniques have made truly impressive inroads against the curse of dimensionality, none have been formally shown

to defeat exponential scaling, none have yet been implemented on massively parallel supercomputers, and none are designed to compute the extremely large numbers ($K \approx 10^4$ – 10^6) of dynamically relevant vibrational (i.e., nuclear motion TI) states that characterize large molecular systems ($f \approx 10$ –30).

In contrast, an alternate exact QD strategy, based on a phase space formalism, has been gaining attention in recent years^{16–31}—particularly because it can formally defeat exponential scaling, does have a massively parallel implementation, and has been used to compute 10^4 – 10^6 states at once.^{24,25} The basic rationale behind the PS approach is very straightforward. Like VSCF, it employs truncation of a primitive DPB, in order to exploit correlation. In such a context, however, it does not suffice to consider only position correlation across the $x_{i,\alpha}$; physics teaches us that dynamical correlation extends across all PS variables—i.e., the $x_{i,\alpha}$ and the $p_{i,\alpha}$. To exploit this correlation to the fullest extent possible, therefore, we need a basis and a truncation scheme that operate on PS, rather than CS. Conversely, it can be shown that any method that does not exploit full PS correlation must formally scale exponentially with system dimensionality, f.

That said, I emphasize at the outset that formal scaling properties are one thing, but practical performance is quite another. Depending on various factors such as the degree of coupling and anharmonicity, the spectral range of interest, $E \leq E_{\text{max}}$, the desired number of computed quantum energy levels, K, and the desired accuracy, ϵ , there are certainly many situations in practice where competing methods can outperform the PS strategies described in this article. However, the opposite is also true, and so the real challenge is to identify a priori those circumstances under which a given method is likely to be the most competitive. To this broader end, also, an analysis based on PS ideas turns out to be extremely beneficial.

The goals of this paper, then, are three-fold. First and foremost, I aim to present a brief review of the use of phase-space-lattice (PSL) basis sets in computational QD, as well as other basis sets that are truncated using PS means. More than a mere history, I compare and contrast these methods with respect to scaling, accuracy, and implementation, in order to establish a set of practical guidelines as to which should be used when. Throughout this discussion, I attempt to make a distinction between what is known mathematically vs. what appears to be suggested from the numerical evidence currently available.

Second, very recently, other researchers^{28,31} have become interested in applying two specific PSL methods invented by the present author^{18,21,22} in the context of extremely highly

accurate calculations—for which the relative error, ϵ , is only one part in 10^{-8} – 10^{-14} . This is much beyond the scope originally intended for use by these techniques. Consequently, the expansion coefficients needed to construct basis functions for the "weylet" PSL method (see Sec. IIB)—originally published over a decade ago¹⁸—are no longer sufficiently accurate to meet current demand. I therefore repeat the calculation of these coefficients to much higher precision—and also provide a correspondingly more complete set of tables.

Third, I present some preliminary results pertaining to the application of PSL (and other) ideas to the realm of electron QD. In particular, several low-lying electronic states of the He atom are computed. In traditional electronic structure, a calculation of just the ground He state might be performed, using some higher-order improvement to Hartree-Fock. In the PSL approach, multiple electronic states are computed directly, in the full six-dimensional (6D) electronic CS, treating electron correlation exactly. The PSL approach is therefore highly relevant for electron QD. I first proposed this idea in 2003—using PS truncation of a particular type of PSL basis called an "affine wavelet". However, the idea was not actually implemented until recently, by D. Tannor and coworkers. These authors did indeed observe remarkable reductions in the required basis size, N, as predicted. However, they considered only 1D model calculations, and also used unrealistic "softened" Coulomb PESs to bypass the Coulombic singularity. In this work, I consider only the true Coulomb interaction—operating only in the full 6D space.

II. BACKGROUND AND THEORY

A. Wigner-Weyl Formalism and the Classical Phase Space Picture

The most rigorous way to apply PS ideas to quantum systems is to invoke a true PS formulation of quantum mechanics. The Wigner-Weyl (WW) formalism^{16,36} provides a one-to-one correspondence between Hermitian quantum *operators*, and real-valued *functions* on the classical PS, $(\mathbf{x}_1, \mathbf{x}_2, \dots, \mathbf{p}_1, \mathbf{p}_2, \dots)$. For example, Hamiltonian operators of the standard kinetic-plus-potential form get transformed as follows:

$$\hat{H} = \sum_{i} \frac{\hat{\mathbf{p}}_{i} \cdot \hat{\mathbf{p}}_{i}}{2m_{i}} + V(\hat{\mathbf{x}}_{1}, \hat{\mathbf{x}}_{2}, \dots) \to H(\mathbf{x}_{1}, \mathbf{x}_{2}, \dots, \mathbf{p}_{1}, \mathbf{p}_{2}, \dots) = \sum_{i} \frac{\mathbf{p}_{i} \cdot \mathbf{p}_{i}}{2m_{i}} + V(\mathbf{x}_{1}, \mathbf{x}_{2}, \dots)$$
(1)

A single wavefunction, Ψ , is transformed via its pure-state density matrix, $\hat{\rho} = |\Psi\rangle\langle\Psi|$:

$$\hat{\rho} = |\Psi\rangle\langle\Psi| \to W_{\Psi}(\mathbf{x}_1, \mathbf{x}_2, \dots, \mathbf{p}_1, \mathbf{p}_2, \dots)$$
(2)

The pure-state "Wigner function," W_{Ψ} , is a quasi-probability distribution function on PS, whose integration over the momentum variables, $(\mathbf{p}_1, \mathbf{p}_2, \ldots)$, results in the usual probability density on CS, i.e. $|\Psi(\mathbf{x}_1, \mathbf{x}_2, \ldots)|^2$. If Ψ is a Hamiltonian eigenstate with energy E, one might well imagine that W_{Ψ} will tend to be largest where $H(\mathbf{x}_1, \mathbf{x}_2, \ldots, \mathbf{p}_1, \mathbf{p}_2, \ldots) \leq E$ —i.e., in the classically allowed region of PS.

Actually, a much stronger statement can be made. Let

$$\hat{\rho}_K = \sum_{k=0}^{K-1} |\Psi_k\rangle \langle \Psi_k| \tag{3}$$

be the density operator that projects onto the lowest K eigenstates of \hat{H} . Further, let k < k' imply $E_k < E'_k$, and $E_{\text{max}} \approx E_K$. Then, the corresponding mixed-state projection Wigner function, W_K , is approximately given by

$$W_K(\mathbf{x}_1, \mathbf{x}_2, \dots, \mathbf{p}_1, \mathbf{p}_2, \dots) \approx \Theta[E_{\text{max}} - H(\mathbf{x}_1, \mathbf{x}_2, \dots, \mathbf{p}_1, \mathbf{p}_2, \dots)], \tag{4}$$

with the approximation become increasingly accurate in the classical limit, $E_{\text{max}} \to \infty$. In other words, the Wigner function for the sum over the K desired states of interest approaches a uniform distribution over the corresponding classical PS.

The relation of Eq. (4) above is of great importance, for it offers the promise of using the classical H to optimize the basis representation of the quantum \hat{H} . The relation itself, as well as various applications to basis set optimization, $^{32-35}$ follow from the derivation of what is called the "classical PS picture." The basic idea is not new, going back at least as far as the Thomas-Fermi model of an electron gas. However, various aspects were developed during my time as a researcher with John C. Light. Fig. 1 is reprinted from an article from that era. In parts (a) and (b), respectively, we see the classical PS region represented by the right-hand-side of Eq. (4), and the corresponding exact quantum $W_K(x, p)$, for the lowest K = 20 states of the harmonic oscillator.

An important aspect of the classical PS picture is that the volume occupied by the classical PS is equal to $K(2\pi\hbar)^f$ —i.e., it is proportional to the number of quantum states, K. For a given calculation, in addition to the desired eigenstates $\Psi_{k < K}$, there is also the representational basis set $\Phi_{n < N}$, which is associated with its own PS region of volume $N(2\pi\hbar)^f$.

The challenge, then, is to choose the Φ_n such that the representational PS region matches the desired PS region as closely as possible. In practice, N must always be larger than K, in order to encompass quantum tunneling beyond the classical PS region. However, if the choice of basis, Φ_n , is sufficiently flexible that it can capture all of the PS correlation, then in principle, one should find that $(N/K) \to 1$ in the large N (or large E_{max}) limit—a property known as perfect asymptotic efficiency. ^{17–19,21,22} Moreover, if the latter property holds for all f, then one also has, de facto, a method that defeats exponential scaling.

To the author's knowledge, the earliest attempt to achieve this goal in the QD context was made by M. Davis and E. Heller (D&H), in a remarkable 1979 paper. ¹⁶ Specifically, they proposed using H and E_{max} to truncate a rectilinear lattice of PS Gaussians (PSGs) distributed at "critical density"—i.e., one per $(2\pi\hbar)^f$ Planck cell. (D&H also considered other densities, and other, nonrectilinear arrangements of PSGs). In 1D, each PSG function, g_{mn} , is labeled with two integer indices, rather than one. The first is the position index, m, and the second is the momentum index, n. The center of the PSG Wigner function is thus located at the PS point, $(m\sqrt{2\pi\hbar}, n\sqrt{2\pi\hbar})$. The generalization for arbitrary f is straightforward. The above PSL approach promises perfect PS flexibility—i.e., the ability to capture all PS correlation. Moreover, PSG's offer the most localized W_{Ψ} functions possible, suggesting that the PSGs should be more efficient than any other choice of PSL basis function. Yet, the method proved to be far less effective than expected.

In retrospect, the difficulties of the D&H approach are due to two issues:

- 1. PSGs are non-orthogonal, and so unlike for Eq. (3), $W_N \neq \sum_{mn} W_{g_{mn}}$ (in 1D).
- 2. The Balian-Low "no-go" theorem^{18,38,39} essentially precludes *any* critically-dense rectilinear PSL of identical PS-translated basis functions, Φ_{mn} (in 1D), from being amenable to effective PS truncation.

Regarding 1., even though the individual PSGs are very localized, there is a *collective* non-locality that effectively emerges, because the correct density matrix is given by

$$\hat{\rho}_N = \sum_{k=0}^{N-1} \sum_{l=0}^{N-1} |g_k\rangle \left[\tilde{S}^{-1}\right]_{kl} \langle g_l| \tag{5}$$

instead of by Eq. (3). In Eq. (5), \tilde{S} is the overlap matrix—i.e., $\tilde{S}_{kl} = \langle g_k | g_l \rangle$, where k and l are composite indices, each representing a set of $(m_{i \leq f}, n_{i \leq f})$ index pairs (for arbitrary

f). The mixed-state Wigner function for the collection of N PSGs is therefore not a simple sum of individual Wigner functions, but also involves "coupling" of well-separated PSGs. Regarding 2., the situation—and its resolution—are a bit more subtle.

B. Successful Rectilinear Phase Space Lattice Techniques

The difficulties described in Sec. II A above can be overcome. In a 2003 paper,¹⁷ I presented the first QD method that formally defeats exponential scaling, and also achieves perfect asymptotic convergence—the so-called "weylet" approach. It was soon applied to model systems as large as f = 15.^{18,19} Later, my graduate student R. Lombardini proposed the closely related, but simpler "symmetrized Gaussian" (SG) approach,²¹ which has since been applied to a variety of real and model systems up to f = 27, including methyleneimine and acetonitrile.^{22–24} Both weylet and SG are rectilinear PSL (RPSL) approaches. Of all the PSL methods described in this article, the SG approach is by far the simplest to implement numerically. This is at least true for force-field PESs, for which all SG matrix elements are known analytically—although a scalable quadrature method for more general PESs has also been developed.²⁰

Addressing issue 1. from Sec. II A above, the weylet approach applies a simple Löwdin canonical orthogonalization procedure, ^{18,40} which replaces the non-orthogonal g_k PSG basis with a corresponding orthogonalized PSL basis, Φ_k , that spans the same space:

$$|\Phi_k\rangle = \sum_{l} \left[\tilde{S}^{-1/2} \right]_{kl} |g_l\rangle \tag{6}$$

With regard to issue 2., we note that the Balian-Low theorem applies only to RPSL basis functions on a critically dense lattice. One solution, therefore, is to work with a set of doubly dense (in 1D) RPSL functions, from which orthogonal basis functions are then constructed as a linear combination of one positive-momentum function (m, n > 0), and the corresponding (m, -n) negative-momentum function. This necessitates the use of half-integer rather than integer n indices, as indicated in Fig. 2. In any event, these measures give rise to an orthonormal weylet RPSL basis, for which Eq. (3) applies—and moreover, one for which the individual Φ_k basis functions decay exponentially with respect to distance from their PS centers.^{18,41}

Numerical implementation of the weylet method requires an explicit summation of the

form of Eq. (6). In principle, this summation is *infinite*, which ensures that the resultant $|\Phi_k\rangle$ are perfect PS-translated copies of each other, and also that the same universal expansion can be used for all applications. In practice, only a finite summation is required, as the expansion coefficients decay exponentially with |l-k| (Sec. III A). Note that explicit matrix inversion is *not* required for each new calculation. Instead, the 1D inverse square root overlap matrix, $\tilde{S}^{-1/2}$, has been computed once for all time, and is presented in Sec. III A. The generalization for arbitrary f is straightforward, as this is just a direct product of 1D matrices. Moreover, the exponential decay in coefficient values now applies across *all* dimensions at once, which greatly reduces the total number of terms that must be considered explicitly.

In the weylet procedure as described above, the first step is to apply the summation in order to generate the doubly-dense RPSL functions, and the second step is to apply momentum symmetrization to obtain the final orthogonal weylet basis. On the other hand, it is also possible to bypass the summation step altogether, and work directly with momentum-symmetrized doubly-dense PSGs. This is exactly the SG approach. The resultant SG basis functions are not orthogonal; yet, they still avoid the collective non-orthogonality problem of the D&H approach, to the extent that they are nearly as efficient as weylets for most applications (at least for large f; see Sec. III A).

There are also other avenues for getting around the Balian-Low no-go theorem. Again, the theorem technically applies only to a critically dense RPSL of (1D) basis functions, Φ_{mn} , that are perfect PS-translated copies of each other. One simple way to modify the D&H PSGs to remove the PS-translation property is to apply a Fourier low-band-pass filter projection to each g_{mn} . In other words each PSG is projected onto the space spanned by momentum eigenstates in the range $-p_{\text{max}} \leq p \leq p_{\text{max}}$.

The above strategy characterizes the so-called "pvb" and related methods of Tannor and coworkers. ^{26–28} In practice, rather than projecting directly on momentum states, one uses a set of orthonormal sinc functions, which span the same banded Fourier space. Moreover, a Fourier projection *per se* is not essential; in principle, the desired effect can be achieved using other projection subspaces. ³⁰ However, most work to date has been done using Fourier projections, and it is convenient to think along these lines.

If p_{max} is sufficiently large, the above projection will not adversely impact the accuracy of the computed results. Moreover—with Balian-Low evidently in check—the resultant projected PSG basis is now amenable to effective PS truncation. This must be im-

plemented carefully, as the projected PSG functions (denoted \tilde{g}_{mn}) are not orthogonal, and so Eq. (5) applies, rather than Eq. (3). However, by introducing the *dual functions*, $|\tilde{b}_k\rangle = \sum_{l=0}^{N-1} \left[\tilde{S}^{-1}\right]_{kl} |\tilde{g}_l\rangle$, one can replace Eq. (5) with the form $\sum_{k=1}^{N-1} |\tilde{b}_k\rangle\langle\tilde{g}_k|$, which resembles Eq. (3). This form suggests that the *dual* representation should be amenable to effective PS truncation, as is indeed found to be the case. Moreover, due to well-known properties of sinc representations (or more generally, any basis set corresponding to Gaussian quadrature^{42,43}), the representational error decays as a *Gaussian*, outside of the classical PS region.

In comparison with the weylet and SG methods, the numerical implementation of pvb requires that an explicit overlap matrix inversion be performed for each new calculation—an additional computational step not required by weylet/SG. However, the pvb method can be implemented in such a manner that this \tilde{S} inversion does not become the computational (CPU) bottleneck of the whole calculation (for the untruncated basis, the inversion can be applied to each dimension separately, as discussed above).

Ample numerical evidence suggests that pvb achieves perfect asymptotic efficiency in 1D. Although it is likely that pvb also formally defeats exponential scaling, this has yet to be established mathematically. Regardless of its formal scaling properties, the N values required for simple pvb to achieve convergence for larger f may be beyond reach, in practice. To the author's knowledge, ²⁸ the largest systems to which pvb or related methods have been applied are for f = 6—as compared with f = 27 for SG. This marked difference in scalability is likely due to the fact that pvb uses a critically-dense, rather than a doubly-dense RPSL—and is therefore characterized by a 2^f -fold loss in resolution, as compared to the weylet/SG approach. On the other hand, once the convergence regime is reached, pvb is expected to converge to high accuracy substantially faster than weylet/SG, owing to the Gaussian vs. exponential decay (see Sec. III A).

C. Other Large-f Applications of the Phase Space Picture

Quite distinct from its associations with the above RPSL methods, the PS picture also presents a useful and versatile analytical tool, with respect to maximizing the performance of just about any QD basis set, especially at large f. As discussed in Sec. I, one common strategy to mitigate the curse of dimensionality is to apply correlated truncation to a DPB

of the form $\Phi_{k_1,...k_f}(x_1,...x_f) = \varphi_{k_1}^{(1)}(x_1) \times \cdots \times \varphi_{k_f}^{(f)}(x_f)$ (where the α subscript is now suppressed). In this manner, correlations can be exploited across the full f-dimensional parameter space of 1D basis functions, $(k_1,...,k_f)$ —if not across the full 2f-dimensional PS. Even though such a strategy does not formally defeat exponential scaling, it can still lead to tremendous reductions in N for large f.

Typically, the 1D basis functions, $\varphi_{k_i}^{(i)}(x_i)$ are energy-like eigenfunctions of 1D effective Hamiltonians, $\hat{H}_{i \leq f}$, with energies $E_{k_i}^{(i)}$. The \hat{H}_i are often taken to be harmonic oscillators (HOs), with $E_{k_i}^{(i)} = \hbar \omega_i (k_i + 1/2)$. For systems characterized by polynomial force field PESs with small anharmonicity and mode coupling, HO basis sets provide very good results at the bottom of the energetic spectrum. This approach is used, e.g. in the MULTIMODE package¹⁵ developed by J. M. Bowman and coworkers—although more general VSCF basis sets can also be employed.

Regardless of the particular choice of basis, the primary question is the following: how should the correlated truncation of the $\varphi_{k_i}^{(i)}(x_i)$ be optimized, so as to provide the most accurate eigenenergies at the bottom of the spectrum—or at some other desired spectral locale? For f = 1, there is only one sensible choice, i.e., $k \leq k_{\text{max}}$. For large f, the number of reasonable-seeming truncations of $(k_1, \ldots k_f)$ space is vast—as is, also, the corresponding range in performance. Clearly, it would be worthwhile to have an a priori guide, describing which correlated truncation scheme should be applied when—yet surprisingly little effort has been expended in this direction.

For the simplest and most widely-used scenarios, the PS picture provides us with a simple and reliable set of rules. Consider separable correlated truncations of the general form,

$$\sum_{i=1}^{f} \alpha_i k_i \le k_{\text{max}},\tag{7}$$

where k_{max} is the sole convergence parameter. The problem of choosing an optimized truncation scheme then reduces to that of choosing the weights, α_i , so as to maximize the accuracy of the desired computed eigenvalues. Two natural choices emerge. First, if $\hat{H} = \sum_{i=1}^f \hat{H}_i$ truly were a separable HO, then perfect results (i.e., N = K, with all states computed to infinite precision) would be obtained by setting $\alpha_i = \hbar \omega_i$ and $k_{\text{max}} = E_{\text{max}}$. We refer to this choice as "frequency-weighted" truncation (FWT)—since the individual weights, and the entire sum itself, have units of frequency/energy. In the opposite limit, we have $\alpha_i = 1$ (for all i), for which k_{max} is an integer, representing the total number of excitations summed

over all i. The latter choice is termed "polyad" truncation (PT), since the individual weights, and the sum, are integers. Clearly, there are many other "intermediate" choices that could also be considered.

The PS picture provides the desired answers by explicitly considering quantum tunneling beyond the classically allowed PS region.^{24,25} In particular, it reveals that PT is the most efficient choice at the bottom of the energy spectrum—followed by intermediate weighting schemes at higher energies, and then by FWT beyond that. Moreover, the PS picture further predicts that above a certain energy, all HO or DPB correlated truncation schemes give way to weylet/SG as the most effective approach. This is because of coupling and anharmonicity, which necessarily increase with increasing energy, at least for force field PESs.

These trends were all observed explicitly, in a recent calculation of the lowest 10,000 quantum states of acetonitrile (f=12).^{24,44} (Figure 2 depicts a typical phase space "slice" for this system.) In particular, by using a combination of the above methods and correlated truncation schemes, the most accurate spectrum across the entire dynamically relevant range (within 6500 cm⁻¹ of the ground state) was obtained. The performance of this "hybrid" spectrum is indicated in Table I. A more detailed breakdown by individual method is presented in Ref. 24, Fig. 3. As expected, PT is the most efficient choice at the very bottom of the energy spectrum—offering 0.001–0.1 cm⁻¹ convergence for the lowest 100 or so energy levels. For the next 2000 or so levels, the intermediate weighting schemes are best for this system, achieving ~ 1 cm⁻¹ convergence—followed by FWT beyond that, in the ~ 10 cm⁻¹ regime. At still higher energies, the predicted transition to weylet/SG is also observed. Similar ideas were later applied to benzene (f=30), for which one million quantum states were computed (albeit not to very high accuracy).²⁵

III. NEW RESULTS AND DISCUSSION

A. Weylet and SG Calculations at Extremely High Accuracy

In Ref. [21], R. Lombardini and I first proposed the non-orthogonal SG basis, as a choice that offers nearly the same efficiency as the weylet basis but is simpler to implement. We went on to provide a comprehensive investigation of scalability and basis set efficiency. In general, such an investigation requires variation over three separate parameters: (1)

system dimensionality, f; (2) desired relative accuracy threshold, ϵ ; (3) number of converged eigenvalues, K. Such a comparison for weylets vs. SGs may be found in Refs. [21] and [22]. The main conclusion is that, at the large f values of primary interest—where neither approach achieves high accuracy without further refinements—SGs are only slightly less efficient than weylets. As a typical example, for a model f = 14 HO system, with a basis size of N = 24,942 and relative accuracy of $\epsilon = 0.03$, the weylet method achieves K = 1794 states, whereas SG achieves K = 1758.²²

On the other hand, very recent numerical work by other authors^{28,31} has addressed explicitly the case of low f and extremely high accuracy (i.e. $\epsilon \approx 10^{-8}$ – 10^{-14})—comparing the SG and weylet methods to each other, as well as to other techniques. From the numerical data, it appears that in this regime, weylets outperform SGs by a significant margin. It has also been reported that weylets are in turn outperformed by other related techniques, such as pvb. However, these comparisons used the expansion coefficient table reported in Ref. [18], which is only accurate to 10^{-8} or so. A proper comparison, clearly, requires more accurate weylet expansion coefficients, that also extend significantly further out in PS.

In this work, I have used *Mathematica* to recompute all of the relevant weylet expansion coefficients, to 20 digits of precision. All coefficients whose numerical magnitude is greater than 10^{-20} are reported in Tables II and III. The new coefficient values agree with those in Ref. [18], to the precision to which the latter were reported. Therefore, even accounting for substantial compounding of numerical roundoff errors, the new coefficient values should more than suffice for extremely accurate calculations in the ϵ ranges described above. The new values are also available from the author in electronic form, upon request.

I computed the new expansion coefficients as follows.¹⁸ First, I began with the half-dense RPSL of PSGs, centered at the PS origin—or equivalently, the doubly-dense RPSL PSGs that correspond to even values of both m and n. Next, I truncated these PSGs within a square-shaped region, corresponding to $|m| \leq m_{\text{max}}$ and $|n| \leq m_{\text{max}}$. The even-valued quantity m_{max} is the sole convergence parameter. The next step was to create the overlap matrix \tilde{S} from the truncated Gaussians—the dimensions of which are clearly $(m_{\text{max}}+1)^2 \times (m_{\text{max}}+1)^2$. The elements of \tilde{S} were evaluated to 30 digits of precision—which was preserved in the subsequent inverse square root overlap matrix calculation for $\tilde{S}^{-1/2}$. To verify that this level of precision was indeed achieved, I also numerically computed $\tilde{S}^{-1/2} \cdot \tilde{S} \cdot \tilde{S}^{-1/2}$, and confirmed that the resulting product matrix was indeed the identity, to thirty digits of precision.

The Löwdin canonical orthogonalization procedure as described previously has the advantage that it uniquely associates individual orthogonal and non-orthogonal basis functions (unlike, e.g., the Gram-Schmidt procedure⁴²). In principle, one must compute the expansion coefficients for the infinite matrix corresponding to $m_{\text{max}} \to \infty$ —for which all column vectors of $\tilde{S}^{-1/2}$ become identical, PS-translated copies of each other. In reality, edge effects associated with the finite truncation cause small deviations from translational invariance. These deviations should be smallest for the column vectors of $\tilde{S}^{-1/2}$ corresponding to Φ_{mn} centered near the PS origin—i.e., those furthest from the edges. Accordingly, I used the (m=0,n=0) column vector of $\tilde{S}^{-1/2}$ as the $(m_{\text{max}}+1)\times(m_{\text{max}}+1)$ PS expansion coefficients, reported in Tables II and III—exploiting, also, the symmetry with respect to $m\to -m$, $n\to -n$, and $(m,n)\to (n,m)$.

I assessed convergence in two different ways. First, I compared the (m=0,n=0) column vector to the adjacent (PS-translated) (m=2,n=0) column vector obtained from the same m_{max} calculation. This provides a measure of the degree of translation invariance achieved, or the role of edge effects. Second, I compared the (m=0,n=0) column vector for the largest m_{max} calculation to that of a slightly smaller m_{max} calculation. In the present context, the largest calculation performed was for $m_{\text{max}} = 28$, with $m_{\text{max}} = 24$ used for comparison. With respect to both measures of convergence, the largest discrepancies so obtained were no larger than $\sim 10^{-20}$.

Using the new coefficient values as computed above, one may of course expect to see a marked improvement in weylet performance for extremely high accuracy calculations. On the other hand, it is not likely that this improvement will make up for the full difference in performance with the pvb approach in this regime, as this was reported in Ref. [28]. It is important to understand the likely reasons for this—to which end, a PS analysis is once again very advantageous.

In the weylet approach, because the basis functions are orthogonal, one can directly add/subtract individual W_{Φ_k} 's to W_N , as in Eq. (3). Moreover, it is well-established that the individual weylet Wigner functions exhibit exponential decay, with respect to PS distance (as measured in a certain natural sense^{18,20}) from the weylet center. For computed energy eigenstates up to E_{max} , this implies at best an *exponential* convergence of accuracy, with respect to distance beyond the classical PS region used to retain additional weylet basis functions. On the other hand, the pvb method exploits a "dual" approach, for which the

truncated dual basis functions \tilde{b}_k exhibit *Gaussian* convergence of accuracy—even though they are non-orthogonal, and fairly delocalized in PS.

For the above reason, one may expect the pvb approach to be the more efficient method in the context of low f, and extremely high accuracy. On the other hand, a weylet or SG approach is more efficient than pvb at high f—where high accuracies are beyond the reach of any method, except at the relatively uninteresting region at the bottom of the spectrum. The weylet/SG approach is more efficient in this context because it provides much better sampling resolution of the relevant PS. In particular, because it uses a doubly-dense grid, the resolution is improved by a factor of two per dimension—or by a factor of 2^f in all. Evidently, this difference is what makes it possible to perform weylet/SG calculations up to f = 27, 22,24 whereas pvb-type calculations have to date been extended only up to f = 6.

It must also be borne in mind that the above comparison is for TI calculations only. For TD calculations, the pvb approach has the advantage of not being constrained by momentum symmetry. Whereas it is certainly *possible* to use weylets in a TD context, the momentum symmetry constraint will necessarily lead to reduced efficiency. It is an interesting question—currently being explored by Tannor and coworkers⁴⁵—whether, and more specifically in what contexts, the reduced resolution of the pvb approach is outweighed by its ability to capture momentum asymmetry, in TD applications.

Returning to TI calculations at larger f, it is also worth knowing when one should employ the weylet over the SG approach. Based on the previous discussion, it seems likely that for many applications, there will be an "intermediate" regime—corresponding to perhaps something like f = 4–12 and $\epsilon \approx 10^{-3}$ –10⁻⁶—in which weylets outperform both SGs and pvbs. For much larger f values, neither SG nor weylet (in their simplest implementations as described here) can achieve high accuracy, and so the SG approach is preferred, as it is simpler to implement (though neither SG nor weylet is any more difficult to code than any other PSL method). As discussed in Sec. IIB, the weylet Hamiltonian matrix construction requires summations similar to Eq. (6). It can be shown that the number of CPU operations per matrix element scales as a power law. ^{20–23} The CPU effort required for matrix construction becomes comparable to that of matrix diagonalization when this number approaches $N \approx 700,000$ (the largest explicit matrix size considered to date). For f = 8, this corresponds to $m_{\text{max}} \approx 8$, or (from Tables II and III) an expansion error of $\epsilon \approx 10^{-6}$ —which is still smaller than the expected basis set error.

B. Electron Dynamics: A preliminary investigation

For Coulombic PESs, both the challenges and opportunities of PSL methods appear to be quite different than in the vibrational, nuclear motion context—and are therefore worthy of separate consideration. Regarding opportunities, the concave-shaped PS regions that characterize Coulombic interactions offer the potential for tremendous reduction—even in 1D, but especially as f is increased. Although this aspect was evidently first suggested by the present author, ¹⁸ it was not actually demonstrated until more recent work by Tannor and coworkers ²⁶—who indeed observed a 13–60-fold reduction in N, in 1D. Moreover, the promise of greatly improved efficiency with increasing f is particularly relevant for electron QD applications—for which the conventional single-electron-Hartree-Fock-based techniques that have been so successful in electronic structure, may not be so well suited.

As promising as is this earlier work by Tannor and coworkers, it has been limited in several important respects by the aforementioned technical challenges, which are severe. Foremost among these are the singularities in the PES—which give rise to infinitely tall PS regions at the nuclear positions, even for bound electronic states. This is how the "cusp problem" manifests in a PS treatment. With respect to a rectilinear lattice of PSL functions, one can arrange the PS centers so as to avoid a single nuclear position, but it is harder to avoid all nuclei. In many-electron applications, avoiding the electron-electron repulsion singularity is substantially more difficult.⁴⁵

To deal with the above situation, Tannor and coworkers sometimes replace the true PES with a "softened" Coulomb approximation, which has no attractive singularities at the nuclear positions. Additionally, these authors avoid the repulsive singularity by considering only one-electron systems—meaning that the role of electron correlation remains completely unexamined. Finally, they artificially reduce the dimensionality of the Coulomb problem down to just 1D (f = 1)—which could have unphysical ramifications, given that the inverse power law form of the Coulomb PES is inextricably linked to the fact that there are f = 3 spatial dimensions.

In the present work, we (myself and coworker J. Jerke) overcome all of these limitations, in the course of computing several low-lying electronic states of the He atom. The calculations are performed in the full f = 6 quantum dimensionality, using exact Coulombic PESs. Electron correlation is thus treated *exactly*, although for this preliminary study, spin is

ignored. Our numerical calculation thus provides exact non-fine-structure-corrected energy levels and wavefunctions, for both para- and ortho-helium.

Although PS ideas as discussed in this paper are used to truncate the basis, this is not just a simple weylet or SG representation. In order to handle the singularities, we make use of new matrix element integration technology⁴⁶ that applies a Fourier band-pass filter. In addition to this, a tensor product decomposition strategy is also employed. The details of this method will be provided in a future publication. For the present purpose, it suffices to state that all parameters associated with these refinements (e.g., the tensor rank) have been chosen such that their contribution to the total error is significantly less than the largest source of error—which is basis set truncation.

Computed energy levels (frequencies) for the ground (lowest-lying excited) state(s) are presented in Table IV, and compared with experimental data.⁴⁷ All calculations were performed on a single node, with the longest requiring 42 hours of CPU time. For the ground state, both the numerical convergence and the agreement with experiment are to within a few .001 Ha. Note that substantially better convergence may not lead to a commensurate improvement in experimental agreement, as fine structure effects are not considered here. In any event, the computed ground state energy is much closer to experiment than is the Hartree-Fock value⁴⁸ (also presented).

In contrast, the excited state energy levels are less well converged—to one or two .01 Ha, which also characterizes the agreement with experiment. One might have expected a tremendous reduction in accuracy as compared with the ground state—due to the much larger CS region explored by the 2s or 2p electron, by virtue of its excitation and greater screening. On the other hand, the corresponding PS region increase is much more modest, as a consequence of which the resultant loss in accuracy (less than a single digit) is mitigated significantly. Even more encouraging, however, is the fact that excited state frequencies are significantly more accurate than energy levels. The frequencies in Table IV, obtained from a separate calculation designed to optimize the latter, are converged to just a few .001 Ha.

All in all, the numerical performance is quite good, considering that the calculation was performed directly in the full f = 6 quantum dimensionality, treating all electron correlation explicitly. Evidently, there is extensive correlation across all twelve PS variables, $\mathbf{x}_1, \mathbf{x}_2, \mathbf{p}_1$, and \mathbf{p}_2 , which the method is able to exploit. Some of this "correlation" (in the broad, PS sense) is clearly evident in Fig. 3, which presents various two-dimensional integrated density

plots for the computed electronic ground state wavefunction. Note that electron correlation (i.e., "correlation" in the electronic structure sense) accounts for much of this.

As a final comment, I point out that our procedure as implemented above, does not as yet make any special allowances for the cusp. Traditional electronic structure methods use ever-narrowing Gaussian functions, to deal effectively with cusps. Alternatively, in a PSL context, I proposed¹⁸ (and D. Tannor has implemented²⁶) using affine rather than PS-translated wavelets. Affine wavelets are related to each other via width rescaling, as well as CS translation—rendering them highly suitable for cusp regions. As of yet, neither affine wavelets, nor traditional Gaussians, have been incorporated into our PSL calculation of the He electronic states, as described above. However, either or both of these refinements could be implemented, no doubt leading to further improvements in performance.

IV. SUMMARY AND CONCLUSIONS

For decades, computational chemists and molecular physicists have wrestled with the "curse of dimensionality"—treating all degrees of freedom explicitly quantum mechanically, in the context of nuclear motion dynamics. Similar challenges may apply in the emerging field of electron dynamics. Whether the context is nuclear or electronic, if accurate "quantum dynamics" calculations for large systems is the goal, then this goal cannot be achieved without first facing down the curse of dimensionality head-on.

Phase space offers a very promising avenue for doing just that. In particular, the classical phase space picture as discussed in Sec. II A provides a clear understanding of the exponential scaling that underlies the curse: both where it comes from, and how to eradicate it. Indeed, this picture was used to develop the first quantum dynamics method formally known to defeat exponential scaling—i.e., the weylet method, as discussed in Secs. II B and III A. Moreover, it has inspired other, related methods, such as SG and pvb. Collectively, these methods have been successfully applied in circumstances that seemingly lie beyond the capabilities of other state-of-the-art techniques. In particular, I know of no other methods that can compute all of the extremely large number of vibrational states (e.g., $K \approx 10^4$ – 10^6) that become dynamically relevant when f is large.

On the other hand, the phase space methods also have their own limitations—such as a profound difficulty in achieving high accuracy when f is large. Here, too, the phase space

picture provides a quantitative understanding of why and how this is the case—albeit in a more refined version, that describes the quantum tunneling of Wigner functions beyond the classical phase space region implied by Eq. (4). This more refined picture also tells us when each of the various rectilinear phase space lattice methods considered here is likely to be the most effective—e.g., SG for the largest f and largest f calculations, weylet for intermediate f and f, and finally, pvb for the smallest, but most accurate calculations (and also, explicitly time-dependent applications). The refined phase space picture also provides an extremely useful analysis of conventional basis set methods. Few basis sets are less basic or more widely used than the harmonic oscillator—particular in molecular vibration applications. Yet, until the phase-space analysis of Sec. II C was performed, the optimal means of truncating a harmonic oscillator basis for large f [in accord with Eq. (7)] was evidently not known.

Returning to the three rectilinear phase space lattice methods discussed in this article—i.e., weylet, SG, and pvb—the assessments as drawn above and in Secs. IIB and III should decidedly not be considered closed. All three approaches are still under active development, with various beneficial refinements being introduced to improve accuracy, performance, and scalability. The major goal is to improve the accuracy for large f—a challenge that requires improving the Wigner representation, near and beyond the edge of the classical phase space region at $H = E_{\text{max}}$. One effective strategy, at least for small f, is to project individual weylet or SG basis functions using phase space region operators²¹—reminiscent of the Fourier projection in pvb, but applied here for an entirely different purpose. A more straightforward approach that has been explored by several authors is to employ a non- E_{max} -based phase space truncation criterion, when growing the representational basis of N functions beyond the first K that correspond to the classical region. E_{max} -three projections in the second content of the representational basis of E_{max} -based phase space truncation criterion, when growing the representational basis of E_{max} -based phase

It is also possible to merge aspects of the different methods together. For example, Tannor and coworkers have recently explored the "pW" approach^{28,45}—i.e., weylet basis functions that have been band-pass projected—which seems to offer some advantages. Indeed, a similar strategy is adopted in Sec. III B. Other refinements, to better accommodate quadrature, overlap matrix inversion, iterative eigensolvers, tensor products, massive parallelization, etc., are also being considered. To this list we must also add "singular potentials"—for it seems that the integration and other technologies employed in Sec. III B have now, for the first time, opened the door to performing calculations for real electrons, using phase space lattice

methods. This new development could prove very significant for electron dynamics. In any event, whatever the future may bring, it seems clear that phase space ideas will enjoy a bright future in the field of quantum dynamics, for some years to come.

As a final comment, I am very pleased and humbled to be able to say that—insofar as my own contributions in the phase space quantum dynamics arena are concerned—these began during my time as a postdoctoral associate with John C. Light. It was with John that I published most of my early papers on the classical phase space picture,^{32–35} and I will forever be grateful for the opportunity that his group provided me, early in my career, to develop these ideas.

Acknowledgments

The work by the author that was discussed in this article was conducted with research grant support from both The Robert A. Welch Foundation (D-1523) and the National Science Foundation (CHE-0741321). In addition, two instrumentation grants from the National Science Foundation are also acknowledged: CHE-0840493 and PHY-1126251. Some of the calculations presented in this paper were performed using the SWITCHBLADE parallel code, written by T. Halverson. J. Jerke is also acknowledged, for the preliminary electron dynamics calculations. I also gratefully acknowledge the following computational facilities: TTU Department of Chemistry and Biochemistry, Robinson cluster; TTU High Performance Computing Center, Hrothgar facility; Texas Advanced Computing Center, Lonestar facility; Texas Southern University High Performance Computing Center, Ares cluster.

¹ P. A. M. Dirac, The Principles of Quantum Mechanics (Oxford Science Publications, Oxford, UK, 1958).

² J. von Neumann, Mathematical Foundations of Quantum Mechanics (Princeton University Press, New Jersey, 1932).

³ H. Weyl, The Theory of Groups and Quantum Mechanics (Dover Publications, New York, 1950).

⁴ D. Frenkel and B. Smit, *Understanding Molecular Simulations* (Academic, New York, 2002).

⁵ E. J. O'Reilly and A. Olaya-Castro, Non-classicality of the molecular vibrations assisting exciton energy transfer at room temperature, Nat. Commun., 5 (2014), 3012.

- ⁶ D. Huber and E. J. Heller, Generalized Gaussian wave packet dynamics, J. Chem. Phys., 87 (1987), 5302–5311.
- M. Ceotto, S. Atahan, S. Shim, G. F. Tantardini, and A. Aspuru-Guzik, First-principles semiclassical initial value representation molecular dynamics, Phys. Chem. Chem. Phys., 11 (2009), 3861–3867.
- ⁸ S. Habershon, D. E. Manolopoulos, T. E. Markland, and T. F. Miller, III, Ring-polymer molecular dynamics: quantum effects in chemical dynamics from classical trajectories in an extended phase space, Ann. Rev. Phys. Chem., 64 (2013), 387–413.
- ⁹ M. F. Kling and M. J. J. Vrakking, Attosecond electron dynamics, Annu. Rev. Phys. Chem., 59 (2008), 463–492.
- ¹⁰ J. M. Bowman, The self-consistent-field approach to polyatomic vibrations, Acc. Chem. Res., 19 (1986), 202–208.
- G. Avila and T. Carrington, Jr., Using nonproduct quadrature grids to solve the vibrational Schrödinger equation in 12D, J. Chem. Phys., 134 (2011), 054126.
- H.-G. Yu, Two-layer Lanczos iteration approach to molecular spectroscopic calculation, J. Chem. Phys., 117 (2002), 8190–8196.
- W. Chen and B. Poirier, Parallel Implementation of Efficient Preconditioned Linear Solver for Grid-based Applications in Chemical Physics: II. QMR Linear Solver, J. Comput. Phys., 219 (2006), 198–209.
- ¹⁴ H.-D. Meyer, F. Gatti, and G. A. Worth, eds., Multidimensional Quantum Dynamics: MCTDH Theory and Applications (Wiley-VCH, Weinheim, 2009).
- ¹⁵ S. Carter, J. M. Bowman, and A. R. Sharma, The 'MULTIMODE' approach to ro-vibrational spectroscopy, AIP Conf. Proc., 1504 (2012), 465–466.
- M. J. Davis and E. J. Heller, Semiclassical Gaussian basis set method for molecular vibrational wave functions, J. Chem. Phys., 71 (1979), 3383–3395.
- ¹⁷ B. Poirier, Using wavelets to extend quantum dynamics calculations to ten or more degrees of freedom, J. Theo. Comput. Chem., 2 (2003), 65–72.
- B. Poirier and A. Salam, Quantum dynamics calculations using symmetrized, orthogonal Weyl-Heisenberg wavelets with a phase space truncation scheme: II. construction and optimization, J. Chem. Phys., 121 (2004), 1690–1703.
- ¹⁹ B. Poirier and A. Salam, Quantum dynamics calculations using symmetrized, orthogonal Weyl-

- Heisenberg wavelets with a phase space truncation scheme: III. representations and calculations, J. Chem. Phys., **121** (2004), 1704–1724.
- R. Lombardini and B. Poirier, Rovibrational spectroscopy calculations of neon dimer using a phase space truncated Weyl-Heisenberg wavelet basis, J. Chem. Phys., 124 (2006), 144107.
- R. Lombardini and B. Poirier, Improving the accuracy of Weyl-Heisenberg wavelet and symmetrized Gaussian representations using customized phase space region operators, Phys. Rev. E, 74 (2006), 036705.
- T. Halverson and B. Poirier, Accurate quantum dynamics calculations using symmetrized Gaussians on a doubly dense von Neumann lattice, J. Chem. Phys., 137 (2012), 224101.
- ²³ T. Halverson and B. Poirier, Calculation of exact vibrational spectra for P₂O and CH₂NH using a phase space wavelet basis, J. Chem. Phys., **140** (2014), 204112.
- ²⁴ T. Halverson and B. Poirier, Large scale exact quantum dynamics calculations: Ten thousand quantum states of acetonitrile, Chem. Phys. Lett., **624** (2015), 37–42.
- T. Halverson and B. Poirier, One million quantum states of benzene, J. Phys. Chem. A, 119 (2015), 12417–12433.
- A. Shimshovitz and D. J. Tannor, Communication: Phase space wavelets for solving Coulomb problems, J. Chem. Phys. 137 (2012), 101103.
- A. Shimshovitz and D. J. Tannor, Phase-space approach to solving the time-independent Schrödinger equation, Phys. Rev. Lett. 109 (2012), 070402.
- ²⁸ H. R. Larsson, B. Hartke, and D. J. Tannor, Efficient molecular quantum dynamics in coordinate and phase space using pruned bases, J. Chem. Phys. 145 (2016), 204108.
- J. Brown and T. Carrington, Using an iterative eigensolver to compute vibrational energies with phase-spaced localized basis functions, J. Chem. Phys. 143 (2015), 044104.
- J. Brown and T. Carrington, Comment on "Phase-Space Approach to Solving the Time-Independent Schrödinger Equation," Phys. Rev. Lett. 114, (2015), 058901.
- J. Brown and Tucker Carrington, Jr., Assessing the utility of phase-space-localized basis functions: Exploiting direct product structure and a new basis function selection procedure, J. Chem. Phys. 144 (2016), 244115.
- ³² B. Poirier and J. C. Light, Phase space optimization of quantum representations: direct product basis sets, J. Chem. Phys., 111 (1999), 4869–4885.
- ³³ B. Poirier and J. C. Light, Efficient distributed Gaussian basis for rovibrational spectroscopy

- calculations, J. Chem. Phys., 113 (2000), 211–217.
- ³⁴ B. Poirier, Algebraically self-consistent quasiclassical approximation on phase space, Found. Phys., 30 (2000), 1191–1226.
- ³⁵ B. Poirier and J. C. Light, Phase space optimization of quantum representations: Three-body systems and the bound states of HCO, J. Chem. Phys., 114 (2001), 6562–6571.
- M. Hillery, R. F. O'Connell, M. O. Scully, and E. P. Wigner, Distribution functions in physics: fundamentals, Phys. Rep., 106 (1984), 121–167.
- N. H. March, The Thomas-Fermi approximation in quantum mechanics, Adv. Phys., 6 (1957), 1–98.
- ³⁸ R. Balian, Un principe d'incertitude fort en théorie du signal ou en mécanique quantique, C. R. Acad. Sc. Paris, 292 (1981), 1357–1361.
- ³⁹ F. Low, Complete sets of wave-packets, 17–22 A Passion for Physics—Essays in Honor of Geoffrey Chew (World Scientific, Singapore, 1985).
- ⁴⁰ P.-O. Löwdin, Adv. Phys. **5** (1956), 1.
- ⁴¹ I. Daubechies, S. Jaffard, and J.-L. Journé, A simple Wilson orthonormal bases with exponential decay, SIAM J. Math. Anal., **22** (1991), 554–572.
- ⁴² W. H. Press, B. P. Flannery, S. A. Teukolsky, and W. T. Vetterling *Numerical Recipes* (Cambridge University Press, England, 1989).
- ⁴³ R. G. Littlejohn, M. Cargo, T. Carrington, Jr., K. A. Mitchell, and B. Poirier, A general framework for discrete variable representation basis sets, J. Chem. Phys., **116** (2002), 8691– 8703.
- ⁴⁴ D. Bégué, P. Carbonniere, and C. Pouchan, Calculations of vibrational energy levels by using a hybrid ab Initio and DFT quartic force field: application to acetonitrile, J. Phys. Chem. A, 109 (2005), 4611–4616.
- ⁴⁵ D. Tannor (private communication).
- ⁴⁶ J. L. Jerke, Y. Lee, and C. J. Tymczak, A novel Gaussian-Sinc mixed basis set for electronic structure calculations, J. Chem. Phys., 143 (2015), 064108.
- 47 http://www.physics.nist.gov/PhysRefData/Handbook/Tables/heliumtable5.htm
- ⁴⁸ J. Mohallem, Comment on "On the helium ground-state Hartree–Fock energy", Chem. Phys. Lett., **195** (1992), 457–458.

TABLE I: Number of converged energy levels for CH₃NH at varying levels of accuracy, ϵ . Convergence was determined by comparing the second largest calculation (N=480159) to the largest (N=733312). Column I is the error tolerance in cm⁻¹, used to determine which states are "accurately" computed. Column III is efficiency of the basis as determined by comparing the ratio of number of accurate states, K to the basis size, N.

Number of Converged States for CH ₃ CN					
Accuracy (cm ⁻¹)	Number of States (K)	Efficiency $(\frac{K}{N})$			
1000	479173	99.8%			
100	243255	50.7%			
10	10035	2.09%			
1	310	0.0646%			
0.1	54	0.0177%			
0.01	31	0.00646%			
0.001	6	0.00125%			

TABLE II: Gaussian expansion coefficients, c_{mn} , for normalized (but not momentum-symmetrized) "fiducial" weylet, $\Phi_{00}(x) = \sum c_{mn} g_{mn}(x)$, on doubly-dense rectilinear PS lattice. The Gaussian function, $g_{mn}(x)$, is centered in phase space at the lattice site, $(m\sqrt{\pi}, n\sqrt{\pi})$. Both positive and negative values of m and n are included in the expansion. All coefficients larger than 10^{-20} are included here and in Table III—taking into account the index exchange symmetry, $c_{mn} = c_{nm}$.

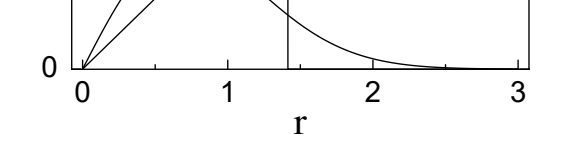
Momentum	Position index $ m $					
index $ n $	0	2	4	6		
0	1.002 814 619 133 862 872 08 -	0.021 713 366 679 443 673 02	2 0.000 703 359 248 430 332 55	-0.000 025 326 890 087 677 42		
2	-0.021 713 366 679 443 673 02	0.000 470 147 007 792 114 70	0 -0.000 015 229 432 217 229 25	$0.000\ 000\ 548\ 388\ 546\ 428\ 14$		
4	0.000 703 359 248 430 332 55 -	-0.000 015 229 432 217 229 25	5 0.000 000 493 325 708 374 47	-0.000 000 017 763 903 753 75		
6	-0.000 025 326 890 087 677 42	0.000 000 548 388 546 428 14	4 -0.000 000 017 763 903 753 75	0.000 000 000 639 650 987 60		
8	0.000 000 957 635 906 854 65 -	0.000 000 020 735 138 074 57	7 0.000 000 000 671 671 572 06	-0.000 000 000 024 185 865 36		
10	-0.000 000 037 244 351 751 09	0.000 000 000 806 430 471 67	7 -0.000 000 000 026 122 633 99	$0.000\ 000\ 000\ 000\ 940\ 636\ 07$		
12	0.000 000 001 475 340 003 95 -	-0.000 000 000 031 944 686 36	6 0.000 000 000 001 034 781 52	-0.000 000 000 000 037 260 90		
14	-0.000 000 000 059 200 996 59	0.000 000 000 001 281 845 04	4 -0.000 000 000 000 041 522 70	0.000 000 000 000 001 495 17		
16	0.000 000 000 002 398 405 38 -	-0.000 000 000 000 051 931 29	0.000 000 000 000 001 682 21	-0.000 000 000 000 000 060 57		
18	-0.000 000 000 000 097 886 26	0.000 000 000 000 002 119 47	7 -0.000 000 000 000 000 068 66	0.000 000 000 000 000 002 47		
20	0.000 000 000 000 004 018 54 -	-0.000 000 000 000 000 087 01	0.000 000 000 000 000 002 82	-0.000 000 000 000 000 000 10		
22	-0.000 000 000 000 000 165 76	0.000 000 000 000 000 003 59	9 -0.000 000 000 000 000 000 12			
24	0.000 000 000 000 000 006 86 -	0.000 000 000 000 000 000 15	5			
26	-0.000 000 000 000 000 000 29					
28	0.000 000 000 000 000 000 01					

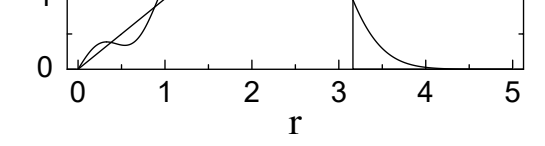
TABLE III: Gaussian expansion coefficients, c_{mn} , for normalized (but not momentum-symmetrized) "fiducial" weylet, $\Phi_{00}(x) = \sum c_{mn} g_{mn}(x)$, on doubly-dense rectilinear PS lattice. See Table II caption for further details.

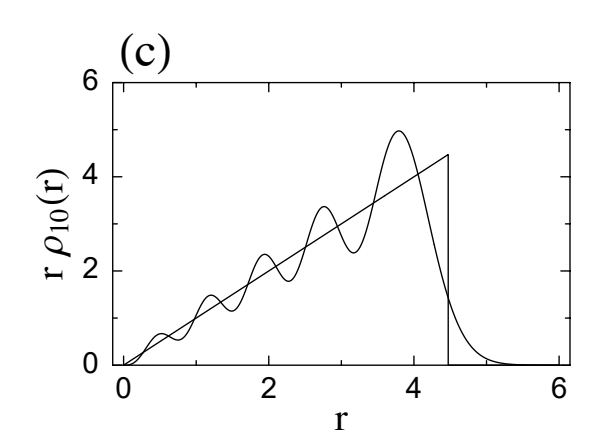
Momentum	Position index $ m $					
index $ n $	8 10 12					
0	$0.000\ 000\ 957\ 635\ 906\ 854\ 65\ -0.000\ 000\ 037\ 244\ 351\ 751\ 09 0.000\ 000\ 001\ 475\ 340\ 003\ 95$					
2	$ -0.000\ 000\ 020\ 735\ 138\ 074\ 57 0.000\ 000\ 000\ 806\ 430\ 471\ 67\ -0.000\ 000\ 000\ 031\ 944\ 686\ 36$					
4	$0.000\ 000\ 000\ 671\ 671\ 572\ 06\ -0.000\ 000\ 000\ 026\ 122\ 633\ 99 0.000\ 000\ 000\ 001\ 034\ 781\ 52$					
6	$ -0.000\ 000\ 000\ 024\ 185\ 865\ 36 0.000\ 000\ 000\ 000\ 940\ 636\ 07\ -0.000\ 000\ 000\ 000\ 037\ 260\ 90$					
8	$0.000\ 000\ 000\ 000\ 914\ 492\ 58\ -0.000\ 000\ 000\ 000\ 035\ 566\ 42 0.000\ 000\ 000\ 000\ 001\ 408\ 87$					
10	$ -0.000\ 000\ 000\ 000\ 035\ 566\ 42 0.000\ 000\ 000\ 000\ 001\ 383\ 25\ -0.000\ 000\ 000\ 000\ 000\ 0054\ 79 $					
12	$0.000\ 000\ 000\ 000\ 001\ 408\ 87\ -0.000\ 000\ 000\ 000\ 000\ 054\ 79 0.000\ 000\ 000\ 000\ 000\ 002\ 17$					
14	$ -0.000\ 000\ 000\ 000\ 000\ 056\ 53 0.000\ 000\ 000\ 000\ 000\ 002\ 20\ -0.000\ 000\ 000\ 000\ 000\ 000\ 000$					
16	0.000 000 000 000 000 002 29 -0.000 000 000 000 000 000 00					
18	-0.000 000 000 000 000 000 09					

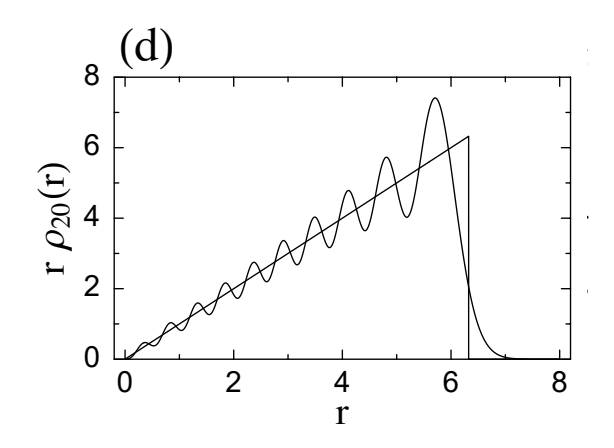
TABLE IV: Ground state energy level and excited state frequencies of the He atom, in Hartrees, as computed using the method described in Sec. IIIB (Column II), and compared with experiment⁴⁷ (Column III). Energy differences are also listed (Column IV). For the ground state energy level, the Hartree-Fock value⁴⁸ is also presented, in the second row. Ground state energies appear above the midrule; excited state frequencies below. Fine structure corrections are *not* included in the calculation. Hence, the three ³P energies (and separately, the three ¹P energies) should be degenerate; the small observed differences are due to numerical errors.

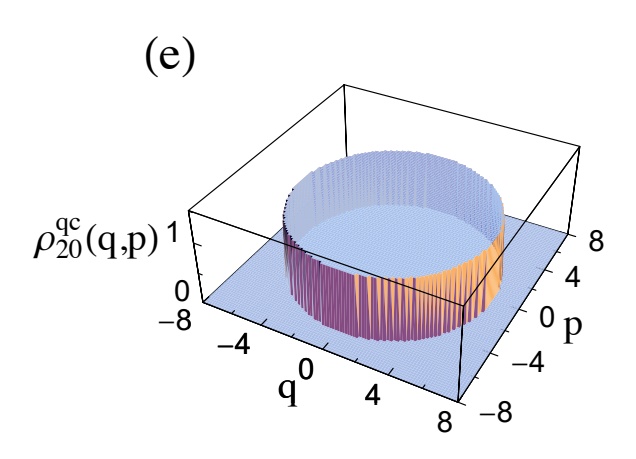
State Label	Computed Energy (Ha)	Experimental Energy (Ha)	Difference (Ha)
$1s^2 (^1S)$	- 2.8968	-2.9037	0.0069
$1s^2$ (HF.)	-2.8617	-2.9037	0.0420
$-1s2s (^{3}S)$	0.7246	0.7284	-0.0038
$1s2s (^1S)$	0.7624	0.7576	0.0048
$1s2p (^3P)$	0.7646	0.7704	-0.0058
$1s2p (^3P)$	0.7649	0.7704	-0.0055
$1s2p (^3P)$	0.7649	0.7704	-0.0055
$1s2p (^1P)$	0.7764	0.7797	-0.0033
$1s2p (^1P)$	0.7765	0.7797	-0.0032
$1s2p (^1P)$	0.7768	0.7797	-0.0029











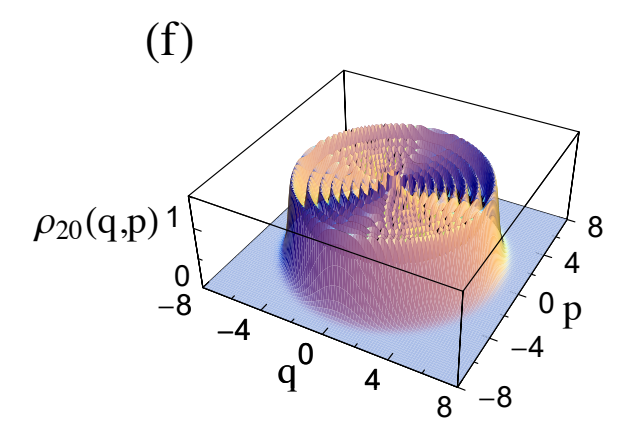


FIG. 2: Schematic representation of doubly-dense weylet/SG RPSL in 1D, for the fourth normal mode of CH₃CN. The gray shaded area is the PS region representing the (eight) basis functions retained via PS truncation—for a calculation of energy states in the dynamically relevant range up to $E_{\rm cut} = 6500 \, {\rm cm}^{-1}$ (outer contour, denoted by thick curve). Source: T. Halverson and B. Poirier, Chem. Phys. Lett. **624** (2015), Fig. 1(b), p. 39. Reproduced with permission of Elsevier.

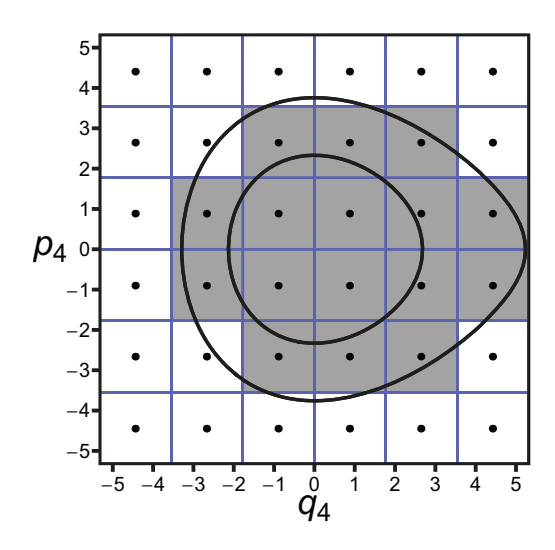


FIG. 3: Contour plots of the electron density for the ground state of the He atom, as computed in Sec. IIIB, and integrated over all but two phase space variables: (a) (x_1, x_2) ; (b) (p_{x_1}, p_{x_2}) ; (c) (x_1, p_{x_2}) . Contours correspond to exponentially-decreasing values of the electron density.

